



# Intramolecularly lactam stapled oxyntomodulin analogues inhibit cancer cell proliferation *in vitro*

Junli Wang<sup>a,b</sup>, Cen Liu<sup>c</sup>, Hongliu Yang<sup>c</sup>, Tao Ma<sup>c</sup>, Yonggang Liu<sup>c</sup>, Fener Chen<sup>a,\*</sup>

<sup>a</sup> Engineering Center of Catalysis and Synthesis for Chiral Molecules, Department of Chemistry, Fudan University, Shanghai 200433, China

<sup>b</sup> Institute of Materia Medica, Chinese Academy of Medical Sciences & Peking Union Medical College, Beijing 100050, China

<sup>c</sup> School of Chinese Materia Medica, Beijing University of Chinese Medicine, Liangxiang Campus, Beijing 102488, China

## ARTICLE INFO

### Article history:

Received 5 September 2022

Revised 8 October 2022

Accepted 18 October 2022

Available online 20 October 2022

### Keywords:

Oxyntomodulin analogues

Intramolecular lactam

Dual GCGR/GLP-1R activations

Anti-PANC-1 proliferation

## ABSTRACT

As a glucagon (GCG) receptor (GCGR) and glucagon-like peptide 1 (GLP-1) receptor (GLP-1R) dual agonist, oxyntomodulin (OXM) has been attracting scientific attentions due to its efficacies of suppressing appetite, increasing energy expenditure, and inducing body weight loss in obese humans. Based on the scaffold of native OXM, specific helix-favoring amino acids substitutions and the consequent salt bridge formations were believed to offer enhanced and balanced GCGR/GLP-1R activations through increasing  $\alpha$ -helical conformation. Novel OXM analogues are obtained by intramolecular lactam stapling of positions [Glu16 & Lys20] or [Lys17 & Glu21] to further strengthen conformationally constrained stabilization. Even though the lactam staple does not provide additional dual GCGR/GLP-1R activations *in vitro*, the stapled OXM analogues are firstly reported to have higher or lower anti-PANC-1 cell proliferation activity, meanwhile which has no obvious inhibitory effect on the proliferation of HeLa cells. Therefore, it is speculated that the stapled analogues may have the potential to inhibit the proliferation of specific cancer cell types. Among the stapled peptides as well as their precursors, analogue **6** has the most prominent anti-PANC-1 proliferation activity with the IC<sub>50</sub> value of 115.1  $\mu$ mol/L. Its mechanism of actions including effective signal pathways should be worth further investigations in future.

© 2023 Published by Elsevier B.V. on behalf of Chinese Chemical Society and Institute of Materia Medica, Chinese Academy of Medical Sciences.

Oxyntomodulin (OXM) is a 37-amino acid peptide enteroendocrine hormone, which is secreted by L-cells of the small intestine in response to nutrient ingestion. It has distinct effects, ranging from regulating glucose metabolism, insulin secretion, to food intake and energy expenditure along with other incretins [1]. Since OXM binds and activates both glucagon (GCG) receptor (GCGR) and glucagon-like peptide 1 (GLP-1) receptor (GLP-1R) *in vitro*, it belongs to a beneficial GCGR/GLP-1R dual agonist. It has been reported that OXM is superior to GLP-1R pure agonist for body weight loss and glucose lowering effects in several preclinical studies, as the dual receptor activations could maximize the efficacies herein [2].

Meanwhile, the activities of native OXM to activate GCGR and GLP-1R *in vitro* were much weaker than the natural ligands [3,4]. Structural modifications, e.g., site mutations, were generally adopted to increase receptor bindings and activations [5–8]. In our previous studies, specific substitutions by helix-favoring amino acids and the consequent salt bridge formations based on the

scaffold of native OXM were believed to offer enhanced and balanced GCGR/GLP-1R activations through increasing  $\alpha$ -helical conformation [9]. So, it is quite interesting and challenging to explore the highly constrained OXM analogues with intramolecular lactam stapling instead of non-covalent salt bridge [10]. Obviously, the covalent lactam stapling in the middle of peptide sequence provides much more strengthened and stabilized  $\alpha$ -helicity than the non-covalent salt bridge, that is supposed to enhance binding affinities to each receptor [2,11].

As OXM could also regulate glucose metabolism, stimulate insulin secretion, suppress food intake, and increase energy expenditure, it has become a prospective target for treating metabolic diseases. Most of native OXM as well as modified analogues have been frequently reported to be applied in the fields of anti-diabetes and/or anti-obesity in pre-clinic and clinic tests [12–14]. Interestingly, native OXM was also reported to inhibit the activation of the NF- $\kappa$ B pathway and then attenuate neuropathic pain induced by TNF- $\alpha$  [15]. In addition to type 2 diabetes and obesity, novel synthetic OXM derivative, cotadutide, with balanced dual agonisms was reported to significantly decrease liver fat, liver volume and diameter in early phase studies, indicating that it may have the potential to be a disease-modifying therapy for nonal-

\* Corresponding author.

E-mail address: [rfchen@fudan.edu.cn](mailto:rfchen@fudan.edu.cn) (F. Chen).

**Table 1**  
Sequences and homology display of OXM, GCG, GLP-1, and exendin-4.

Peptides	Sequence
OXM	<u>HSQGT</u> <sup>10</sup> <u>FTSDY</u> <sup>10</sup> SKYLD <sup>15</sup> SRRAQ <sup>20</sup> <u>DFVQW</u> <sup>25</sup> LMNT K <sup>30</sup> RNRNN <sup>35</sup> IA <sup>37</sup>
GCG	<u>HSQGT</u> <sup>10</sup> <u>FTSDY</u> <sup>10</sup> SKYLD <sup>15</sup> SRRAQ <sup>20</sup> <u>DFVQW</u> <sup>25</sup> LMNT
GLP-1	<u>HAEGT</u> <sup>10</sup> <u>FTSDV</u> <sup>10</sup> SSYLE <sup>15</sup> GQAAK <sup>20</sup> <u>EFLAW</u> <sup>25</sup> LKVG R <sup>30</sup>
Exendin-4	<u>HGEGT</u> <sup>10</sup> <u>FTSDL</u> <sup>10</sup> SKQME <sup>15</sup> EEAVR <sup>20</sup> <u>LFI EW</u> <sup>25</sup> LKNG G <sup>30</sup> PSSGA <sup>35</sup> PEPS <sup>39</sup>

coholic steatohepatitis (NASH) [16]. Furthermore, albumin-binding OXM derivative, S3-2, was identified to improve renal injury in mice through activating GLP-1R and GCGR [17]. However, almost negligible literature is available on the role of any OXM-based activity of anti-cancer *in vitro*, much less *in vivo*.

Recent studies have disclosed the close correlations of type 2 diabetes to the higher incidence, accelerated progression, and increased aggressiveness of many different cancers, such as breast, colon, pancreatic, liver, endometrial, bladder and non-Hodgkin's lymphoma [18]. Moreover, various cancers are hormone-dependent and cross-linked to metabolic alterations, which also significantly increase the frequent occurrence of cancers observed in diabetic patients. The co-occurring properties of hyperglycemia and insulin resistance further consolidate the connections of diabetes and cancers, especially hormone-dependent types [19]. As previously reported by our group, the modified OXM analogue with enhanced and balanced dual receptor activations was observed to exhibit significant hypoglycemic effects along with more insulin stimulation and much improved insulin resistance *in vivo* [9]. So, we are very interested in the exploration of cancer cell assays for the analogues, especially the highly constrained analogues with intramolecular lactam stapling.

Herein, we report the synthesis and biological cancer cell evaluations of a set of novel OXM analogues highly constrained by intramolecular lactam stapling in the middle of peptide sequence. One specific OXM analogue with lactam stapling is firstly observed to have the prominent anti-PANC-1 proliferation activity with the IC<sub>50</sub> value of 115.1 μmol/L. Therefore, it is speculated that the stapled analogues may have the potential to inhibit the proliferation of specific cancer cell types. Its mechanism of actions including effective signal pathways should be worth further investigations in future.

As described in Table 1, OXM comprises the entire 29-amino acid sequence of GCG as well as a C-terminal octapeptide extension (IP-1 tail, intervening peptide, highlighted in blue), and displays high sequence homologies (bold and underlined) with other incretin peptides, GLP-1 and exendin-4. According to the results disclosed previously, 2-aminoisobutyric acid (Aib) at position 2 induced subsequent peptide stability against dipeptidyl peptidase IV (DPPIV) hydrolysis, and Glu16-Lys17-Lys20-Glu21 were the best substitutive residues for the middle sequence of the target peptide. Furthermore, one modified analogue containing IP-1 tail and the other containing truncated C-terminal decapeptide of exendin-4 moiety (30-39, CEX, highlighted in green, Table 1) were both identified to have enhanced and balanced dual receptor activations (~40% and 60%, respectively) through chimeric peptide sequence design [9]. These two analogues were preferably selected as the lead peptides for the intramolecular lactam stapling in this paper. The covalent lactam stapling in the middle of peptide sequence offers much more strengthened and stabilized α-helicity than the non-covalent salt bridge, which is expected to further enhance activations to each receptor.

Based on the descriptions above, a set of analogues were prepared accordingly with native OXM (analogue **1**) sequence as a

**Table 2**  
Sequences of the modified OXM analogues with intramolecular lactam.

No.	Sequence (X = Aib)
1	HSQGT <sup>10</sup> FTSDY <sup>10</sup> SKYLD <sup>15</sup> SRRAQ <sup>20</sup> DFVQW <sup>25</sup> LMNTK <sup>30</sup> RNRNN <sup>35</sup> I A <sup>37</sup> -NH <sub>2</sub>
2	H <b>X</b> QGT <sup>10</sup> FTSDY <sup>10</sup> SKYLD <sup>15</sup> <b>E</b> KRA <b>K</b> <sup>20</sup> EFVQW <sup>25</sup> LMNTK <sup>30</sup> RNRNN <sup>35</sup> I A <sup>37</sup> -NH <sub>2</sub>
3	H <b>X</b> QGT <sup>10</sup> FTSDY <sup>10</sup> SKYLD <sup>15</sup> <b>E</b> KRA <b>K</b> <sup>20</sup> EFVQW <sup>25</sup> LMNTK <sup>30</sup> RNRNN <sup>35</sup> I A <sup>37</sup> -NH <sub>2</sub>
4	H <b>X</b> QGT <sup>10</sup> FTSDY <sup>10</sup> SKYLD <sup>15</sup> <b>E</b> KRA <b>K</b> <sup>20</sup> <b>E</b> EFVQW <sup>25</sup> LMNTK <sup>30</sup> RNRNN <sup>35</sup> I A <sup>37</sup> -NH <sub>2</sub>
5	H <b>X</b> QGT <sup>10</sup> FTSDY <sup>10</sup> SKYLD <sup>15</sup> <b>E</b> KRA <b>K</b> <sup>20</sup> EFVQW <sup>25</sup> LMNT <b>G</b> <sup>30</sup> <b>P</b> SSGA <sup>35</sup> <b>P</b> S <sup>37</sup> -NH <sub>2</sub>
6	H <b>X</b> QGT <sup>10</sup> FTSDY <sup>10</sup> SKYLD <sup>15</sup> <b>E</b> KRA <b>K</b> <sup>20</sup> EFVQW <sup>25</sup> LMNT <b>G</b> <sup>30</sup> <b>P</b> SSGA <sup>35</sup> <b>P</b> S <sup>37</sup> -NH <sub>2</sub>
7	H <b>X</b> QGT <sup>10</sup> FTSDY <sup>10</sup> SKYLD <sup>15</sup> <b>E</b> KRA <b>K</b> <sup>20</sup> <b>E</b> EFVQW <sup>25</sup> LMNT <b>G</b> <sup>30</sup> <b>P</b> SSGA <sup>35</sup> <b>P</b> S <sup>37</sup> -NH <sub>2</sub>

template. Fmoc Rink-amide resin (1%DVB, 100–200 mesh, substitution at 0.34–0.44 mmol/g, Tianjin Nankai Hecheng Sci. & Tech. Co., Ltd.) was exploited as the solid support. Temporary *N*-amino group was protected by Fmoc, which was readily removed by freshly prepared 20% (v/v) piperidine in dimethylformamide (DMF). All the protected amino acids, along with equimolar *O*-(6-chloro-1-hydrocibenzotriazol-1-yl)-1,1,3,3-tetramethyluronium hexafluorophosphate (HCTU) as the coupling reagent, were pre-filled in the independent cartridges. Acyl activation *in situ* was accomplished with two-fold molar excess of *N,N*-diisopropylethylamine (DIEA) in DMF within a couple of minutes. The acylation reactions were performed for 20 min by nitrogen bubble with 6-fold excess of activated amino acid relative to free amines of the resin. After finishing the last cycle on machine, the obtained resin was collected for selective deprotection of Alloc and OAll groups through the reagent of Pd(PPh<sub>3</sub>)<sub>4</sub> in the presence of dichloromethane. Intramolecular lactam stapling was accomplished by the coupling reagents of benzotriazol-1-yl-oxytripyrrolidino-phosphonium hexafluorophosphate (PyBOP) and DIEA.

Cleavage of peptides from the resin was achieved by 95% trifluoroacetic acid (TFA), 2.5% 1,2-ethanedithiol (EDT), and 2.5% water (v/v) for 2 h at room temperature. After filtration, the peptide was precipitated with cold ethyl ether, centrifuged, washed twice with fresh cold ether, dried, resuspended in 5% acetic acid/20% acetonitrile/water (v/v), and lyophilized. Analytical analysis was conducted in 0.1% (v/v) TFA with an acetonitrile gradient on a Waters Xterra@MS system by using C18 column (50 mm × 2.1 mm). The crude peptides were purified by reverse-phase HPLC on a GE AKTA purifier 100 system via a Vydac C4 or C8 column (2.2 mm × 25 cm) in 0.1% (v/v) TFA using a linear gradient of acetonitrile. Fractions containing the desired peptide were pooled and lyophilized. The purity of each analog was confirmed by analytical HPLC analyses (Area% > 95%, details see the Supporting information).

All the modified analogues with detailed site substitutions were exhibited in Table 2. In the same way, 2-aminoisobutyric acid (Aib) substituted at position 2 merely induces peptide stability against dipeptidyl peptidase IV (DPPIV), and does not interfere with recognitions and activations of the dual receptors. Besides the highly reserved residues of Glu16-Lys17-Lys20-Glu21, analogue **2** containing IP-1 tail was the first lead peptide selected for intramolecular lactam stapling. The two bold and double underlined residues indicated the formation for lactam. The lactam stapling between Glu16 and Lys20 produced analogue **3**, and the lactam stapling between Lys17 and Glu21 produced analogue **4**, respectively. Following the same rationale, analogue **5** containing truncated CEX moiety was selected to offer analogue **6** and analogue **7** in parallel.

All the modified analogues were tested *in vitro* for its ability to stimulate cAMP induction in Chinese hamster ovary (CHO) cells over-expressing mGCGR or mGLP-1R. Cells were cultured in

**Table 3**  
Bioactivities of OXM analogues in mGCCR and mGLP-1R.

Analogue	mGCCR			mGLP-1R		
	EC <sub>50</sub> (nmol/L)	SD	Relative (%)	EC <sub>50</sub> (nmol/L)	SD	Relative (%)
Glucagon	0.35	0.03	100	/		
GLP-1	/			0.22	0.03	100
<b>1</b>	5.83	0.46	6.0	12.10	4.05	1.8
<b>2</b>	1.01	0.09	34.6	0.64	0.10	34.3
<b>3</b>	0.84	0.12	41.6	0.54	0.13	40.7
<b>4</b>	0.96	0.10	36.5	0.61	0.08	36.0
<b>5</b>	0.52	0.06	67.3	0.34	0.02	64.7
<b>6</b>	0.49	0.07	71.4	0.30	0.04	73.3
<b>7</b>	0.51	0.06	68.6	0.33	0.03	66.6

minimum essential medium (MEM, Gibco) supplemented with 10% (v/v) fetal bovine serum (FBS, Gibco) at 37 °C, 5% CO<sub>2</sub>. After cell seeding and cell lysate preparation, 40 μL of each analogue was placed in appropriate wells. The cAMP concentrations in each sample were tested by following the manufacturer's instruction. Detect the fluorescence signal at Ex 490 nm and Em 530 nm. Convert the fluorescence signal to cAMP concentration by the cAMP standard curve. The dose-response curve and EC<sub>50</sub> value were plotted and calculated by GraphPad Prism version 7.0 for windows (GraphPad Software, Inc. La Jolla, CA). The results were shown in Table 3. Quite similar to the previously disclosed, the two lead peptides, analogue **2** and analogue **5** were both observed to have comparable and balanced dual receptor activations, demonstrating the truncated CEX moiety should be better than IP-1 tail for dual activities. Their lactam stapled derivatives exhibited similar but a little bit better profiles to their precursors. Obviously, the stapled analogues with truncated CEX moiety still show better dual receptor activations than the stapled analogues with IP-1 tail. Especially, the lactam formation between Glu16 and Lys20, analogue **6**, shows the best dual receptor activations.

Even though the lactam stapling did not significantly enhance receptor activations *in vitro* as expected, all the analogues were secondarily evaluated in two kinds of cancer cell assays, HeLa cell and PANC-1 cell as well.

The PANC-1 pancreatic cancer cells or HeLa cells in the logarithmic growth phase are suspended at a density of  $4 \times 10^4$  cells/well, then placed in the incubator. After culturing for 24 h, the experimental groups are added with peptides dissolved in DMSO diluted with a medium containing 2% FBS, and the final dose concentration of which are 5, 25 and 125 μmol/L. At the same time, 0.1% DMSO control group and a cell-free blank group are also set up. After culturing the cells for 48 h, 10 μL of CCK-8 reagent is added to each well under dark conditions, followed by being incubated for 4 h in the incubator. The absorbance of each well is directly measured at 450 and 690 nm with a microplate reader to calculate the cell proliferation inhibition rate. There are 3 duplicate holes in each group, and the experiment is repeated for three times. The calculation formula of the cell proliferation inhibition rate is as follows:

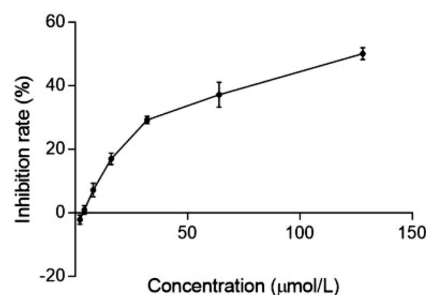
$$\text{Cell proliferation inhibition rate (\%)} = [(A_{\text{control}} - A_{\text{sample}}) / (A_{\text{control}} - A_{\text{blank}})] \times 100\%$$

All absorbance values (A) in the formula are the values obtained by subtracting the reference wavelength (690 nm) from the measured wavelength (450 nm), where the A<sub>control</sub> represents the value of DMSO group, A<sub>blank</sub> represents the absorbance of the culture medium without cells, and the A<sub>sample</sub> represents the absorbance value of the sample.

According to the data obtained, all the analogues did not show any obvious inhibitory effect on the proliferation of HeLa cells unfortunately. Meanwhile, all the peptides showed higher or lower anti-PANC-1 cell proliferation activity with 5-FU as the positive

**Table 4**  
Bioactivities of OXM analogues in HeLa cell and PANC-1 cell.

Analogue	HeLa cell inhibitory rate (%)			PANC-1 cell inhibitory rate (%)		
	5 μmol/L	25 μmol/L	125 μmol/L	5 μmol/L	25 μmol/L	125 μmol/L
5-FU	91.4	89.2	90.9	49.6	59.9	78.6
<b>1</b>	-13.9	-2.0	-1.9	7.6	7.7	19.5
<b>2</b>	0.9	0.9	-27.0	6.0	28.1	34.2
<b>3</b>	-22.7	-0.8	-15.8	7.4	12.9	25.2
<b>4</b>	0.5	-11.6	1.2	15.2	24.7	29.5
<b>5</b>	-14.6	-0.9	3.8	6.8	15.4	28.9
<b>6</b>	-2.0	-4.7	-1.9	9.0	27.0	61.1
<b>7</b>	-6.0	-4.5	-3.5	12.4	22.2	27.1

**Fig. 1.** Dose titration of analogue **6** in anti-PANC-1 cell proliferation assay.

control (Table 4). However, only analogue **6** was observed to exhibit apparent dose dependent manner under the concentrations. Further dose titration indicated that analogue **6** had the most prominent anti-PANC-1 proliferation activity with the IC<sub>50</sub> value of 115.1 μmol/L (Fig. 1). Therefore, it is speculated that the stapled analogues may have the potential to inhibit the proliferation of specific cancer cell types. Its mechanism of actions including effective signal pathways should be worth further investigations in future.

In summary, analogue **6** containing intramolecular lactam stapling, with comparable and balanced dual receptor activations, is firstly observed to have the prominent anti-PANC-1 proliferation activity. It is speculated that the stapled analogues may have the potential to inhibit the proliferation of specific cancer cell types. Its mechanism of actions including effective signal pathways should be worth further investigations in future.

#### Declaration of competing interest

The authors declare that they have no known competing financial interests or personal relationships that could have appeared to influence the work reported in this paper.

#### Supplementary materials

Supplementary material associated with this article can be found, in the online version, at doi:10.1016/j.ccl.2022.107920.

#### References

- [1] D.B. Anderson, J.J. Holst, Peptides 148 (2022) 170683.
- [2] A. Muppidi, H.F. Zou, P.Y. Yang, et al., ACS Chem. Biol. 11 (2016) 324–328.
- [3] A. Poci, P.E. Carrington, J.R. Adams, et al., Diabetes 58 (2009) 2258–2266.
- [4] L.D. Hu, Y.L. Zhang, H. Wang, X.Y. Peng, Y. Wang, Chin. Chem. Lett. 27 (2016) 1027–1031.
- [5] R.C. Camacho, S. You, K.E. D'Aquino, et al., MABS 12 (2020) 1794687.
- [6] W.X. Ding, H.Y. Wang, L.J. Peng, et al., Eur. Rev. Med. Pharm. Sci. 24 (2020) 12423–12436.
- [7] Z.Y. Pei, D.G. Zhou, J. Yan, et al., Life Sci. 253 (2020) 117651.
- [8] P.Y. Yang, H.F. Zou, Z. Amso, et al., Bioconjug. Chem. 31 (2020) 1167–1176.
- [9] T. Ma, S. Huo, B. Xu, et al., Eur. J. Med. Chem. 203 (2020) 112496.
- [10] H. Li, X. Chen, M. Wu, P. Song, X. Zhao, Chin. Chem. Lett. 33 (2022) 1254–1258.
- [11] J.W. Day, N. Ottaway, J.T. Patterson, et al., Nat. Chem. Biol. 5 (2009) 749–757.

- [12] R. Spezani, C.A. Mandarim-de-Lacerda, *Life Sci.* 288 (2022) 120188.
- [13] J.M. Conlon, F.P.M. O'Harte, P.R. Flatt, *Peptides* 147 (2022) 170706.
- [14] J. Tillner, M.G. Posch, F. Wagner, et al., *Diabetes Obes. Metab.* 21 (2019) 120–128.
- [15] Y. Zhang, L.Y. Yuan, Y.B. Chen, C.Y. Lin, G.Y. Ye, *Mol. Med. Rep.* 20 (2019) 5223–5228.
- [16] A. Amblee, *Drugs Future* 45 (2020) 799–811.
- [17] P. Huang, L.Z. Meng, J.H. Tan, et al., *Life Sci.* 270 (2021) 119136.
- [18] S. Tudzarova, M.A. Osman, *Mol. Biol. Cell* 26 (2015) 3129–3139.
- [19] P. Jaiswal, V. Tripathi, A. Nayak, et al., *Curr. Cancer Drug Targets* 21 (2021) 829–848.